glume, which can secondarily alter the fate of the SMs when de-repressed.

None of these models adequately address the fact that the *bd1* SM has different fates in the tassel and ear. It is unlikely that *bd1b* partially compensates for the loss of BD1 in the tassel, as proposed for the *zag1/zmm2* duplication in maize (*14*), because we have been unable to detect *bd1b* transcript in any tissues (*15*). It is possible that a different tassel-specific factor may function redundantly with *bd1*. Given the intense selective pressure on the maize ear, it is not surprising that the ear and tassel are genetically distinct.

The expression pattern and mutant phenotype of *bd1* show similarities to the *FIMBRIATA/UFO* genes of *Antirrhinum* and *Arabidopsis,* respectively (*16*, *17*). Both genes are expressed in a ring at the base of the floral meristem adjacent to the sepals, and the *Antirrhinum* mutant shows a partial loss of lateral determinacy within the meristem. In the case of *UFO*, the basal floral meristems may be replaced with coflorescence branches (*18*). In *Arabidopsis*, the *UFO* and *LEAFY* genes have been proposed to be coregulators of floral meristem identity (*19*). Therefore, BD1 may interact with other SM identity factors to impose determinate meristem fates. As in wild type, the maize *LEAFY* ortholog is expressed in the SPMs and SMs of *bd1* mutants (*5*). However, the genetic interaction between *bd1* and *leafy* is unknown and awaits identification of *leafy* mutants in maize.

To date, *bd1* is the only maize mutant that specifically displays altered SM identity. Several maize mutants that affect SM determinacy have been described, such as *Tassel-seed6* (*20*) and *indeterminate spikelet1* (*21*). Both these mutants display SMs that initiate more than two florets per spikelet, and interestingly, both show normal patterns of *bd1* expression in the SM (fig. S1). The latter result indicates that SM identity is acquired before SM determinacy. Recently, it has been shown that SM identity and determinacy are interdependent, as two genes that control SM determinacy, *indeterminate spikelet1* and *indeterminate floral apex1,* also show SM identity defects as a double mutant (*22*).

The grass spikelet is conventionally interpreted as a strongly contracted branch system—literally, a little spike (*23*). If this interpretation is correct, then genes should exist that, when mutated, cause the spikelet to revert to a branchlike structure. We have identified a gene that regulates spikelet versus branch meristem fates within the inflorescence of maize, and whose sequence and expression are conserved in other grasses such as rice and sorghum. Our data suggest that the expression of *bd1* is fundamental to grass spikelet formation and may have played a role in the origin of this evolutionary novelty.

References and Notes

1. P. McSteen, D. Laudencia-Chingcuanco, J. Colasanti, *Trends Plant Sci.* **5**, 61 (2000).
2. P. C. Cheng, R. I. Greyson, D. B. Walden, *Am. J. Bot.* **70**, 450 (1983).
3. J. H. Kempton, *J. Hered.* **25**, 29 (1934).
4. L. Colombo *et al.*, *Plant J.* **16**, 353 (1998).
5. Materials and methods are available as supporting material at *Science* Online.
6. T. Helentjaris, D. Weber, S. Wright, *Genetics* **118**, 353 (1988).
7. S. Mathews, R. J. Mason-Gamer, R. E. Spangler, E. A. Kellogg, *Int. J. Plant Sci.* **163**, 441 (2002).
8. S. Y. Fujimoto, M. Ohta, A. Usui, H. Shinshi, M. Ohme-Takagi, *Plant Cell* **12**, 393 (2000).
9. J. L. Riechmann, E. M. Meyerowitz, *Biol. Chem.* **379**, 633 (1998).
10. E. van der Graaff, A. D. Dulk-Ras, P. J. Hooykaas, B. Keller, *Development* **127**, 4971 (2000).
11. K. Wilson, D. Long, J. Swinburne, G. A. Coupland, *Plant Cell* **4**, 659 (1996).
12. H. Banno, Y. Ikeda, Q.-W. Niu, N.-H. Chua, *Plant Cell* **13**, 2609 (2001).
13. A. Barkan, R. Martienssen, *Proc. Natl. Acad. Sci. U.S.A.* **88**, 3502 (1991).
14. M. Mena *et al.*, *Science* **274**, 1537 (1996).
15. G. Chuck, unpublished observations.
16. R. Simon, R. Carpenter, S. Doyle, E. Coen, *Cell* **78**, 99 (1994).
17. G. C. Ingram *et al.*, *Plant Cell* **7**, 1501 (1995).
18. J. Z. Levin, E. M. Meyerowitz, *Plant Cell* **7**, 529 (1995).
19. I. Lee, D. S. Wolfe, O. Nilsson, D. Weigel, *Curr. Biol.* **7**, 95 (1997).
20. E. E. Irish, *Am. J. Bot.* **84**, 1502 (1997).
21. G. Chuck, R. Meeley, S. Hake, *Genes Dev.* **12**, 1145 (1998).
22. D. Laudencia-Chingcuanco, *Development* **129**, 2629 (2002).
23. W. D. Clayton, in *Reproductive Versatility in the Grasses*, G. P. Chapman, Ed. (Cambridge Univ. Press, Cambridge, 1990), pp. 32–51.
24. M. Mena, M. A. Mandel, D. R. Lerner, M. F. Yanofsky, R. J. Schmidt, *Plant J.* **8**, 845 (1995).

25. We thank I. Murray, C. Whipple, and M. Ritter for technical assistance, and members of the Hake laboratory and J. Fletcher for comments on the manuscript. This work was supported by grants from the National Science Foundation to R.S. and S.H.

Supporting Online Material

www.sciencemag.org/cgi/content/full/298/5596/1238/DC1
Materials and Methods
Fig. S1

2 August 2002; accepted 17 September 2002

The IκB–NF-κB Signaling Module: Temporal Control and Selective Gene Activation

Alexander Hoffmann,[1]* Andre Levchenko,[2]* Martin L. Scott,[3]† David Baltimore[1]‡

Nuclear localization of the transcriptional activator NF-κB (nuclear factor κB) is controlled in mammalian cells by three isoforms of NF-κB inhibitor protein: IκBα, -β, and -ε. Based on simplifying reductions of the IκB–NF-κB signaling module in knockout cell lines, we present a computational model that describes the temporal control of NF-κB activation by the coordinated degradation and synthesis of IκB proteins. The model demonstrates that IκBα is responsible for strong negative feedback that allows for a fast turn-off of the NF-κB response, whereas IκBβ and -ε function to reduce the system's oscillatory potential and stabilize NF-κB responses during longer stimulations. Bimodal signal-processing characteristics with respect to stimulus duration are revealed by the model and are shown to generate specificity in gene expression.

The transcription factor NF-κB regulates numerous genes that play important roles in inter- and intracellular signaling, cellular stress responses, cell growth, survival, and apoptosis (*1*–*3*). As such, the specificity and temporal control of gene expression are of crucial physiological interest. Furthermore, the realization of the potential of NF-κB as a drug target for chronic inflammatory diseases or within chemotherapy regimens (*4*, *5*) is dependent on understanding the specificity mechanisms that govern NF-κB–responsive gene expression.

Five related mammalian gene products participate in NF-κB functions (RelA/p65, cRel, RelB, p50, p52), but the predominant species in many cell types is a p65:p50 heterodimer. Its activity is largely controlled by three IκB isoforms (IκBα, -β, and -ε) that bind to NF-κB, preventing its association with DNA and causing its localization to the cytoplasm. Signals from various stimuli are transduced to the IκB kinase (IKK) complex, which phosphorylates each IκB isoform, leading to its ubiquitination and proteolysis (*6*). IκB degradation allows NF-κB to translocate to the nucleus and bind DNA (Fig. 1A). The specific role of each IκB protein in regulating NF-κB is not understood. Mice

[1]Division of Biology, California Institute of Technology, Pasadena, CA 91125, USA. [2]Department of Biomedical Engineering, Johns Hopkins University, Baltimore, MD 21218, USA. [3]Department of Biology, Massachusetts Institute of Technology, Cambridge, MA 02139, USA.

*These authors contributed equally to this work.
†Present address: Biogen, Incorporated, Cambridge, MA 02142, USA.
‡To whom correspondence should be addressed. E-mail: baltimo@caltech.edu

with an engineered deletion of one *IκB* gene show notable molecular compensation by the remaining *IκB* family members (*7*, *3*) and mild phenotypes (*8*, *9*). The *IκBα*$^{-/-}$ mouse, however, is perinatal lethal with multi-organ inflammation presumably caused by up-regulation of many NF-κB–responsive genes (*10*, *11*). This phenotype is largely rescued by placing the IκBβ coding region under transcriptional control of IκBα (*12*). IκBα synthesis is controlled by a highly NF-κB–responsive promoter generating autoregulation of NF-κB signaling (*13*).

The interactions of IKK, IκB isoforms, and NF-κB can be thought of as a negative feedback–containing signal-transduction module (Fig. 1A) that receives signals from pathways emanating from cell-surface receptors (input) and transmits signals to nuclear promoter-bound protein complexes regulating gene expression (output). In a minimal system with negative feedback (Fig. 1B), cross-regulation between the two signaling components determines the strength of the negative feedback (constants β and γ) and thus the propensity for oscillations, whereas self-regulation (constants α and δ) determines the degree of damping. Depending on the values of these constants, the response to persistent stimulation may thus vary from continual oscillations, to damped oscillations, to a virtually monotonic rise to a plateau level (Fig. 1B). We examined the dynamics of IκB–NF-κB signaling experimentally by measuring nuclear NF-κB (NF-κBn) activity with the electrophoretic mobility shift assay (EMSA) (*14*). Two phases of NF-κB activation were revealed in response to the stimulation of tumor necrosis factor–α (TNF-α) in various human and mouse cell lines (Fig. 1C). Although the degree and precise timing of postinduction attenuation are variable (*15*, *16*), the output resembles strongly damped oscillations but is distinct from that predicted for a minimal two-component system (Fig. 1B). We conclude that the coordinated degradation, synthesis, and localization of all three IκB isoforms is required to generate the characteristic NF-κB activation profile.

To address their differential functions, we constructed a computational model based on ordinary differential equations. The model behavior depends on the specific values of various control parameters, including those describing (i) the synthesis of each IκB isoform (transcription, mRNA stability, and translation), (ii) the stability of free and NF-κB–bound IκB proteins, (iii) the formation of binary and tertiary IKK–IκB–NF-κB complexes, (iv) the enzymatic rate constants of IKK-containing complexes, and (v) the transport rates affecting localization of each of the components (IκBα, -β, and -ε; NF-κB; and derived complexes). Many of the 30 independent model parameters have been previously determined biochemically, and the values of others may be constrained by published data (*14*). We used reverse genetics to create three IκB–NF-κB signaling modules of reduced complexity and to provide further constraints for effective model parameter fitting.

We engineered mice deleted for *IκBβ* and -ε with the use of standard homologous recombination technology of embryonic stem cells (*14*). These mice, as well as existing *IκBα* gene–deleted mice (*10*), were intercrossed appropriately to yield embryonic fibroblasts in which the nuclear localization of NF-κB was controlled by a single IκB isoform (*14*). TNFα stimulation of fibroblasts that contained only the IκBα isoform resulted in a highly oscillatory NF-κB response, with four equally spaced peaks over the course of the 6-hour experiment (Fig. 2A, top). In contrast, in cells harboring only IκBβ (Fig. 2A, center) or -ε (Fig. 2A, bottom), NF-κBn increased monotonically to a plateau at 1 hour with no notable subsequent repression.

The simplified computational models of β$^{-/-}$ε$^{-/-}$, α$^{-/-}$β$^{-/-}$, and α$^{-/-}$ε$^{-/-}$ cells each contain 17 partially overlapping parameters that control the output, 9 of which have been biochemically determined previously. In addition, five transport parameters are constrained by ratios derived from steady state nuclear and cytoplasmic localization (*17*, *18*). Their absolute values, as well as IκB synthesis parameters, were determined by semiquantitative fitting of the model outputs to the experimental data.

Combining the three models of genetically reduced signaling modules results in a computational model of the IκB–NF-κB signaling module in wild-type cells. Varying their relative contributions revealed discrete functional roles for the mammalian IκB proteins in NF-κB regulation (Fig. 2D). IκBα mediates rapid NF-κB activation and strong negative feedback regulation, resulting in an oscillatory NF-κB activation profile. IκBβ and -ε respond more slowly to IKK activation and act to dampen the long-term oscillations of the NF-κB response. The interplay between these isoforms can result in remarkably rapid responses to the onset or cessation of stimulation and can allow a relatively stable NF-κB response during long-term stimulation (Fig. 2D, middle). In the absence of strong damping mechanisms, high negative feedback efficiency can lead to long-term oscillations in the output (Fig. 2D, top), as observed, for example, in p53-mdm2 cross-regulation (*19*). In wild-type NF-κB signaling, pronounced oscillations are absent and may be detrimental, as *IκBβ*$^{-/-}$*IκBε*$^{-/-}$ females have a dramatically shortened fertility span (*3*). Our results also suggest that varying relative synthesis levels of IκBα, -β, and -ε may constitute a mechanism for altering the responsiveness of the NF-κB signal transduction pathway, a mechanism that cells or cell lineages may use in response to environmental or developmental cues.

To determine the individual contributions of

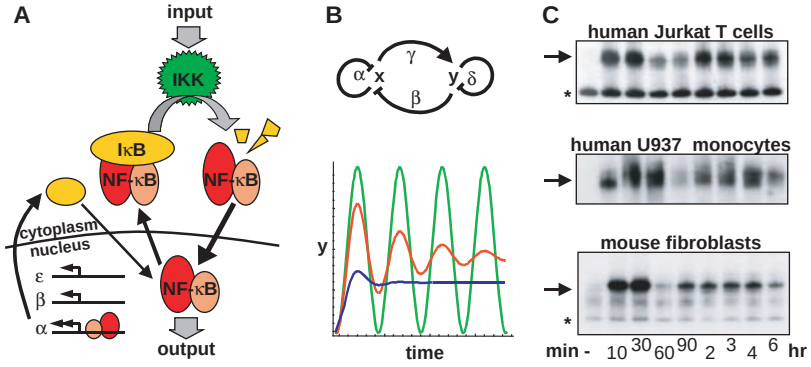

Fig. 1. Negative feedback and the IκB–NF-κB signaling module. (**A**) The IκB–NF-κB signaling module. NF-κB is held inactive in the cytoplasm by three IκB isoforms. Cell stimulation activates the IKK complex, leading to phosphorylation and degradation of IκB proteins. Free NF-κB translocates to the nucleus, activating genes, including IκBα. IκBβ and -ε are synthesized at a steady rate, allowing for complex temporal control of NF-κB activation involving a negative feedback. (**B**) A two-component system (*x* and *y*) with a negative feedback exhibits dynamic behavior that depends on the relative efficiency of the feedback regulation (β and γ) regulating oscillation persistence versus self-regulation (α and δ) causing oscillation damping. This relationship can be described mathematically as $dx/dt = S - \alpha x - \beta y$ and $dy/dt = \gamma x - \delta y$, where S represents the stimulus. The output, *y*, ranges from persistent oscillations (green line, high feedback efficiency and no damping, $\alpha = \delta = 0$), to damped oscillations (red line, intermediate feedback efficiency and intermediate damping), to gradual rising to a plateau level (blue line, low feedback efficiency and high damping). In simulations corresponding to the red line, α and δ are 30% of the respective values used for the generation of the blue line. (**C**) EMSA for NF-κBn in TNFα-stimulated human T cells, human monocytes, and mouse fibroblasts. Nuclear extracts were prepared at the indicated times after the beginning of persistent stimulation with TNFα (10 ng/ml). Equal amounts of nuclear protein were reacted with a radioactively labeled double-stranded oligonucleotide containing a consensus κB site sequence (*14*). Arrows indicate specific nuclear NF-κB binding activity; asterisks indicate nonspecific DNA binding complexes.

the single-IκB isoform models in wild-type fibroblasts, we analyzed nuclear and cytoplasmic extracts during TNF-α stimulation by EMSA for NF-κBn (Fig. 2E, top) and by Western blot for IκB proteins (Fig. 2E, lower panels). NF-κBn first appeared within 5 minutes, as IκBα levels rapidly decreased, and was at its maximum level at 30 min, when cytoplasmic IκBβ and -ε disappeared. After 60 min, κB-binding activity was reduced concomitantly with a transient increase in IκBα protein levels. After 2 hours, NF-κBn returned to about maximum levels and then decreased to about half of maximum levels as IκBα levels stabilized and IκBβ and -ε proteins reappeared. Model-fitting allowed the determination of IκBβ and -ε mRNA synthesis parameters that resulted in an optimal fit of the reconstituted model (Fig. 2F) with experimental wild-type responses. These parameters were about sevenfold lower than those determined for the respective single-IκB models, suggesting previously unrecognized cross-regulation in the expression of IκB genes. The outputs of the resulting "wild-type" model describe NF-κBn (Fig. 2F, top) and cellular IκB isoform levels (Fig. 2F, lower panels) in good qualitative and quantitative agreement with experimental data, thus justifying its use as a predictive tool in experimentation.

We then investigated how transient stimuli control NF-κB activation. Simulated short pulses led to transient NF-κB activation responses, whose duration was insensitive to the duration of the stimulus within the first hour (Fig. 3A). Measuring NF-κBn in transiently stimulated cells confirmed this prediction: TNF-α pulses of 5, 15, 30, and 60 min led to DNA binding activity profiles of similar duration, equivalent to the first peak of persistently stimulated NF-κB activity (Fig. 3B). To explore the signal-processing characteristics of the IκB–NF-κB signaling module, we considered the availability of NF-κBn for binding to an arbitrary κB-responsive promoter. We plotted the duration of NF-κBn availability above an arbitrarily chosen threshold concentration presumed to allow for efficient binding of the κB element of some promoters (Fig. 3C) as a function of the duration of TNF-α stimulation. For long stimulations, NF-κBn lasts as long as the stimulus. For stimulations of less than 1 hour, the duration of the response is largely invariant. Hence, the IκB–NF-κB signaling module has bimodal signal processing characteristics: One mode of signal processing ensures that even short stimulations result in substan-

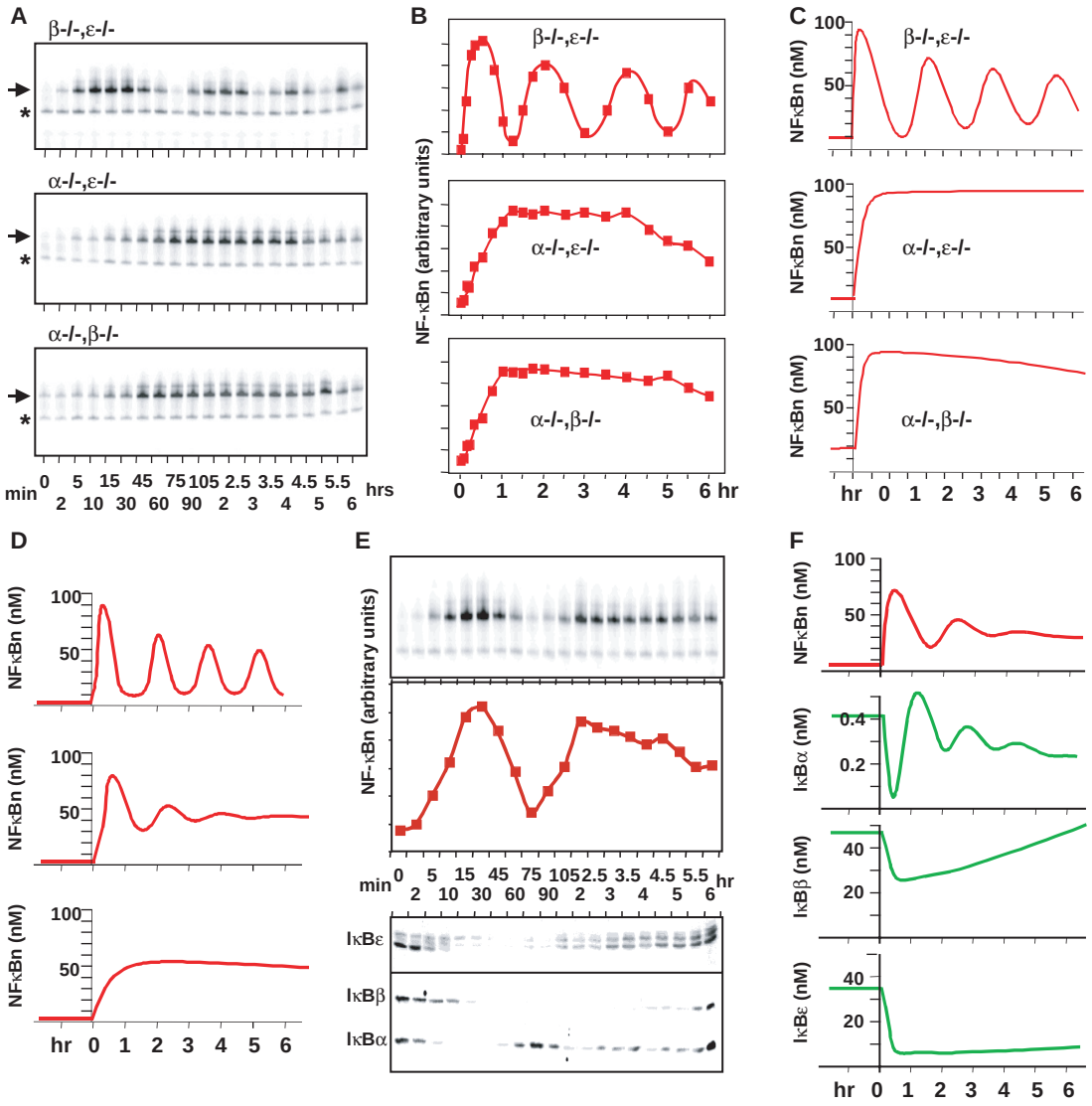

Fig. 2. A computational model based on genetically reduced systems. (**A**) Analysis of NF-κBn by EMSAs of nuclear extracts prepared at indicated times after stimulation with TNF-α (10 ng/ml) of fibroblasts of the indicated genotype. Arrows indicate specific nuclear NF-κB binding activity; asterisks indicate nonspecific DNA binding complexes. (**B**) The NF-κB–specific mobility shift in cells of the indicated genotype was quantitated by phosphoimager and normalized and graphed against a linear time scale. (**C**) Computational modeling of each genetically simplified signaling module results in characteristic kinetics of the NF-κBn response. Model-fitting allows previously undetermined biochemical parameters to be estimated. (**D**) Models of the simplified signaling modules are combined, with increasing IκBβ and -ε transcription rates, while keeping the IκBα transcription rate constant. Model behaviors are shown that result as the constitutive mRNA synthesis parameters for IκBβ and IκBε are increased fivefold (top to middle) and then sevenfold (middle to bottom). The bottom panel represents the NF-κBn output predicted by a model with mRNA synthesis parameters identical to those employed in the single IκB isoform models shown in Fig. 2C. (**E**) Biochemical analysis of NF-κB and IκB isoforms in wild-type fibroblasts. NF-κBn (top) assayed by EMSA at the indicated times after persistent stimulation with TNF-α. The specific NF-κB–specific mobility shift was quantitated by phosphoimager and normalized and graphed at the indicated nonlinear time scale. Western blots of corresponding cytoplasmic fractions are probed with anti-bodies specific to IκBα and -β (bottom) and IκBε (above). (**F**) Verification of the computational model for wild-type cells. IκBα and -β mRNA synthesis parameters were determined by qualitative model fitting to yield the graphed outputs in response to persistent stimulation of NF-κBn (top) and total cellular concentrations of IκBα, -β, and -ε (lower panels as indicated).

tial NF-κB responses; the other mode, operative at stimulations longer than 1 hour, generates responses proportional in duration to the stimulus.

One implication of the above-described temporal regulatory switch is that some NF-κB–responsive genes might be efficiently activated by a stimulation pulse as short as 15 min (Fig. 4A, blue stippled line). However, there may be other genes that require longer (>1 hour) exposure to NF-κB. We tested this hypothesis by examining the behavior of two NF-κB–regulated genes that display different transcriptional activation profiles (*3*). One gene encodes the chemokine IP-10, which displays detectable mRNA levels within 30 min of TNF-α stimulation (Fig. 4B) (*14*). A 15-min pulse of TNF-α was sufficient to activate IP-10 transcription, although, as might be expected, persistent stimulation yielded greater amounts of IP-10 mRNA at later time points. In contrast, the chemokine gene RANTES required at least 2 hours of stimulation for detectable expression and was not induced by a shorter, transient stimulation (Fig. 4B). The model predicts that in cells lacking IκBα, NF-κB will have a longer nuclear lifetime after a short TNF-α pulse (Fig. 4A, red lines) than in wild-type cells. Indeed, transient stimulation led to an extended peak of κB-binding activity, similar to responses resulting from longer stimulations (compare upper panels in Fig. 4, B and C). In turn, RANTES gene transcription was induced not only with persistent stimulation but also with transient stimulations as short as 15 min in IκBα$^{-/-}$ cells (Fig. 4C).

Thus, the bimodal temporal signal-processing characteristics of the IκB–NF-κB module result in not only quantitative but also qualitative regulation of gene expression defining two classes of genes: those that require persistent NF-κB activation and those that do not. The latter genes (e.g., IP-10) undergo a standard activation program irrespective of the precise duration of a transient TNF-α stimulus. IκB–NF-κB signal processing ensures that even very short stimulations can produce easily detectable transcriptional activation of such genes. Conversely, the former genes (e.g., RANTES) may or may not require expression of NF-κB–induced transcription factors with which NF-κB must synergize for gene induction. RANTES induction is protein synthesis–independent (*3*), and although the mechanism for the apparent delay in RANTES induction is unknown, it is noteworthy that histone H4 acetylation in macrophages was shown to be lipopolysaccharide-inducible on the RANTES promoter while it was constitutive on many other chemokine promoters (*20*). If H4 acetylation, a marker for chromatin accessibility, precedes NF-κB binding to the endogenous promoter, it may be induced by a NF-κB–independent pathway. Our results imply that specificity in gene expression can be achieved by using two signal transduction pathways in temporally distinct ways. Gene induction only occurs when the two pathways are temporally coordinated.

Our analysis has revealed the IκB–NF-κB signaling module as a biological system that regulates cellular behavior through the control of system dynamics. The generation of genetically reduced systems enabled the computational analysis of complex dynamic behavior. Exploration of the computational model, in turn, provided insights into the physiologically relevant differential functions of heretofore seemingly redundant system components. Their distinct but coordinated regulation in synthesis and degradation allows for a transcriptional response system with signal-processing characteristics that exhibit both rapid signal responsiveness and stable long-term responses.

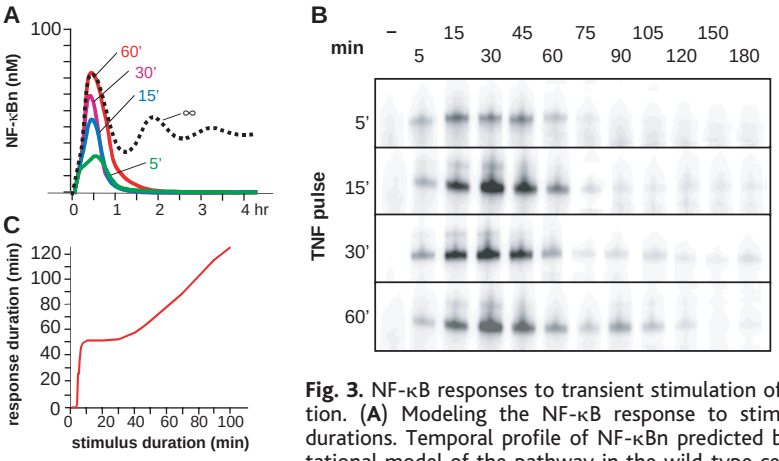

Fig. 3. NF-κB responses to transient stimulation of varying duration. (**A**) Modeling the NF-κB response to stimuli of various durations. Temporal profile of NF-κBn predicted by the computational model of the pathway in the wild-type cells in response to stimulations of the same intensity but varying durations as indicated. (**B**) Experimental NF-κBn data for transient TNF stimulation regimes. Each panel shows the results from EMSAs with nuclear extracts after the onset of a transient stimulation with TNF-α for 5, 15, 30, and 60 min. (**C**) Graph of the duration of above-threshold (20 nM) NF-κBn as a function of the duration of the transient stimulus as predicted by the computational model.

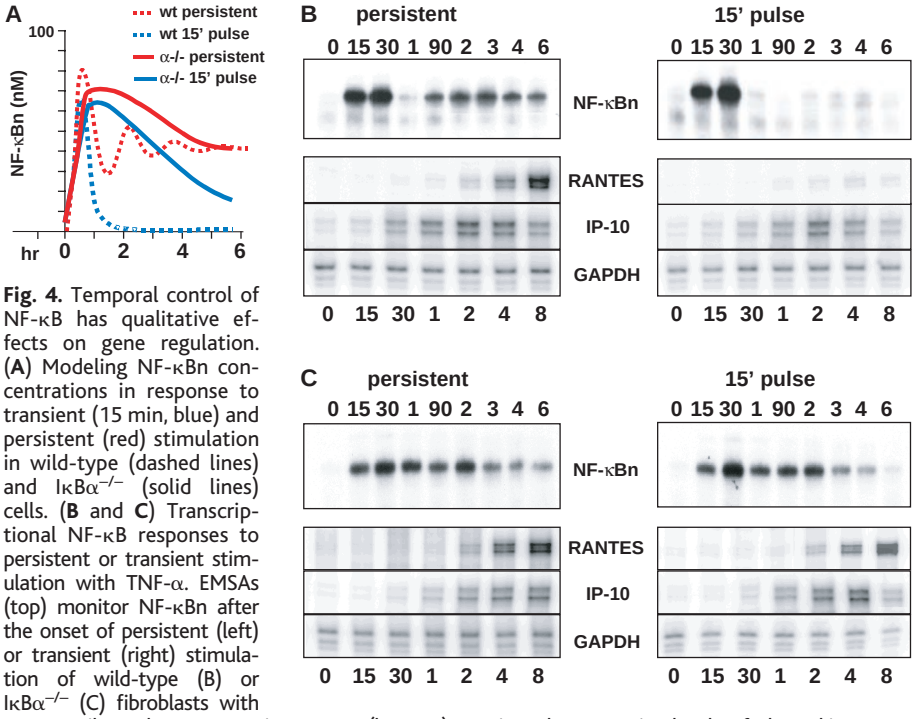

Fig. 4. Temporal control of NF-κB has qualitative effects on gene regulation. (**A**) Modeling NF-κBn concentrations in response to transient (15 min, blue) and persistent (red) stimulation in wild-type (dashed lines) and IκBα$^{-/-}$ (solid lines) cells. (**B** and **C**) Transcriptional NF-κB responses to persistent or transient stimulation with TNF-α. EMSAs (top) monitor NF-κBn after the onset of persistent (left) or transient (right) stimulation of wild-type (B) or IκBα$^{-/-}$ (C) fibroblasts with TNF-α. Ribonuclease protection assays (bottom) monitor the transcript levels of chemokine genes RANTES and IP-10 as well as the housekeeping gene glyceraldehyde phosphate dehydrogenase (GAPDH) at indicated times (in min and hours) after the onset of persistent (left) or transient (right) stimulation of wild-type (B) or IκBα$^{-/-}$ (C) fibroblasts with TNF-α.

References and Notes

1. S. Gerondakis, M. Grossmann, Y. Nakamura, T. Pohl, R. Grumont, *Oncogene* **18**, 6888 (1999).
2. H. L. Pahl, *Oncogene* **18**, 6853 (1999).
3. A. Hoffmann, D. Baltimore, unpublished results.
4. P. P. Tak, G. S. Firestein, *J. Clin. Invest.* **107**, 7 (2001).
5. Y. Yamamoto, R. B. Gaynor, *J. Clin. Invest.* **107**, 135 (2001).
6. S. Ghosh, M. J. May, E. B. Kopp, *Annu. Rev. Immunol.* **16**, 225 (1998).
7. S. T. Whiteside, J. C. Epinat, N. R. Rice, A. Israel, *EMBO J.* **16**, 1413 (1997).
8. S. Memet *et al.*, *J. Immunol.* **163**, 5994 (1999).
9. M. L. Scott, D. Baltimore, unpublished results.
10. A. A. Beg, W. C. Sha, R. T. Bronson, D. Baltimore, *Genes Dev.* **9**, 2736 (1995).
11. J. F. Klement *et al.*, *Mol. Cell. Biol.* **16**, 2341 (1996).
12. J. D. Cheng, R. P. Ryseck, R. M. Attar, D. Dambach, R. Bravo, *J. Exp. Med.* **188**, 1055 (1998).
13. M. L. Scott, T. Fujita, H. C. Liou, G. P. Nolan, D. Baltimore, *Genes Dev.* **7**, 1266 (1993).
14. Materials and methods are available as supporting material on *Science* Online.
15. I. Kemler, A. Fontana, *Glia* **26**, 212 (1999).
16. Y. Han, T. Meng, N. R. Murray, A. P. Fields, A. R. Brasier, *J. Biol. Chem.* **274**, 939 (1999).
17. F. Carlotti, S. K. Dower, E. E. Qwarnstrom, *J. Biol. Chem.* **275**, 41028 (2000).
18. W. F. Tam, R. Sen, *J. Biol. Chem.* **276**, 7701 (2001).
19. R. LevBarOr *et al.*, *Proc. Natl. Acad. Sci. U.S.A.* **97**, 11250 (2000).
20. S. Saccani, S. Pantano, G. Natoli, *J. Exp. Med.* **193**, 1351 (2001).

21. The authors thank T. L. Johnson, S. Sanjabi, S. Smale, R. Tanaka, and an anonymous reviewer for suggestions on the manuscript. A.H. gratefully acknowledges the Jane Coffin Child Foundation for Cancer Research for postdoctoral fellowship support.

Supporting Online Material

www.sciencemag.org/cgi/content/full/298/5596/1241/DC1
Materials and Methods
SOM Text

15 March 2002; accepted 28 August 2002

The Neurotrophin Receptor p75^{NTR} as a Positive Modulator of Myelination

José M. Cosgaya,* Jonah R. Chan,* Eric M. Shooter†

Schwann cells in developing and regenerating peripheral nerves express elevated levels of the neurotrophin receptor p75^{NTR}. Neurotrophins are key mediators of peripheral nervous system myelination. Our results show that myelin formation is inhibited in the absence of functional p75^{NTR} and enhanced by blocking TrkC activity. Moreover, the enhancement of myelin formation by endogenous brain-derived neurotrophic factor is mediated by the p75^{NTR} receptor, whereas TrkC receptors are responsible for neurotrophin-3 inhibition. Thus p75^{NTR} and TrkC receptors have opposite effects on myelination.

The neurotrophin receptor p75^{NTR} (*1*) is now known to have more diverse functions than that of being a helper for the Trk receptors. We show that the brain-derived neurotrophic factor (BDNF) acts through p75^{NTR} to enhance myelin formation. The neurotrophins, a family of growth factors including nerve growth factor (NGF), BDNF, neurotrophin-3 (NT3), and neurotrophin-4/5 (NT4/5), exert their biological actions mostly in neuronal cells by regulating survival, differentiation, and cell death (*2*). All known neurotrophins bind the receptor p75^{NTR}, but others of the Trk family of tyrosine kinase receptors are more selective about which neurotrophin they will bind. NGF binds to TrkA, BDNF and NT4/5 bind to TrkB, and NT3 binds to TrkC. Alternative splicing of the *trkB* and *trkC* genes results in full-length receptor isoforms (TrkB-FL and TrkC-TK$^+$) that contain an intact tyrosine kinase domain and the truncated isoforms (TrkB-T1 and -T2 and TrkC-TK$^-$) that lack the kinase domain (*3*, *4*).

The myelin sheath is a specialized membrane component in the nervous system that maximizes the conduction efficiency and velocity of neuronal action potentials. The myelination program involves a number of signals between the neuronal and myelin-forming cells that include, in the peripheral nervous system (PNS), neuregulins (*5*), adenosine triphosphate (*6*), steroid hormones (*7*), Desert hedgehog (*8*), and the neurotrophins BDNF and NT3 (*9*). Removal of BDNF inhibited myelination, whereas removal of NT3 enhanced myelination in vitro and in vivo (*9*).

To identify the neurotrophin receptors responsible, we determined which receptor mRNAs were present during myelination both in sciatic nerve and in Schwann cell/dorsal root ganglia neuron (SC/DRG) cocultures by nonquantitative reverse transcription–polymerase chain reaction (RT-PCR). The mRNAs for p75^{NTR} and TrkC-TK$^+$ were present in both actively myelinating sciatic nerve and cocultures (Fig. 1A). TrkB-T1 mRNA was also detected in sciatic nerve and in cocultures, whereas only a minute amount of TrkB-FL was observed. Myelination in the sciatic nerve, determined by the expression of the major myelin

Department of Neurobiology, Stanford University School of Medicine, 299 Campus Drive, Fairchild Building, Stanford, CA 94305, USA.

*These authors contributed equally to this work.
†To whom correspondence should be addressed. E-mail: eshooter@cmgm.stanford.edu

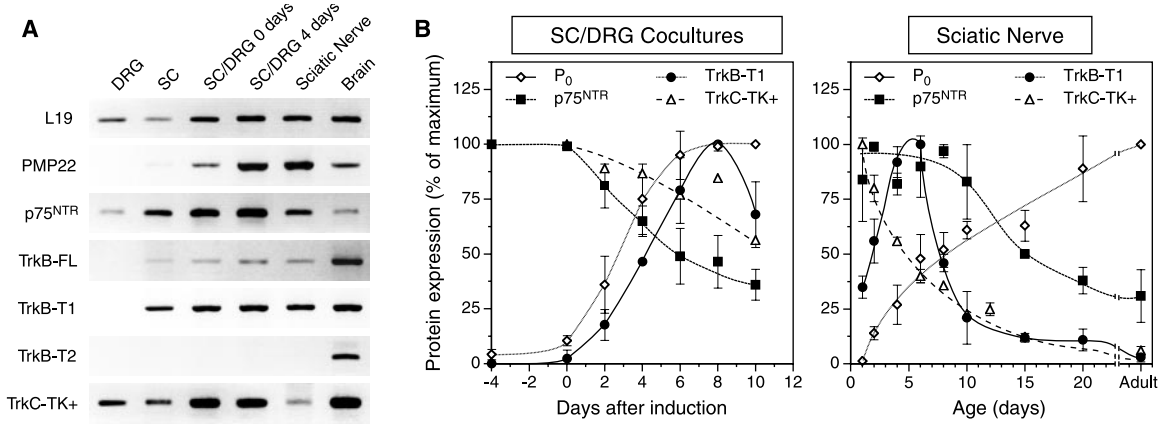

Fig. 1. p75^{NTR}, TrkB, and TrkC are present during development in sciatic nerve and SC/DRG cocultures. (**A**) Expression of neurotrophin receptors, the myelin protein PMP22, and the ribosomal protein L19 was analyzed by RT-PCR from purified rat DRG, SC, premyelinating SC/DRG cocultures before induction of myelination (SC/DRG 0 days), actively myelinating cocultures after 4 days of induction (SC/DRG 4 days), newborn mouse sciatic nerve, and adult mouse brain. (**B**) Protein levels of the myelin protein P_0 and the neurotrophin receptors p75^{NTR}, TrkC-TK$^+$, and TrkB-T1 were analyzed by Western blot in SC/DRG cocultures and in rat sciatic nerve at the times indicated. The results are presented as the mean ± SD.

ERRATUM

Post date 7 December 2007

Reports: "The IκB–NF-κB signaling module: Temporal control and selective gene activation" by A. Hoffmann, *et al.* (8 November 2002, p. 1241). It has come to our attention that Fig. 3B may give the appearance that lanes were spliced or possibly duplicated. The experiments that yielded this figure were carried out in 1997 using autoradiography when the authors were at the Massachusetts Institute of Technology. Similar experiments were rerun after the authors had moved to the California Institute of Technology. Because more stringent standards for handling electronic images have arisen more recently [see, e.g., M. Rossner, K. M. Yamada, *J. Cell Biol.* **166**, 11 (2004)], we provide a recently created figure based on data from a similar experiment (top), as well as an image of the full gel (bottom) captured with a Molecular Dynamics Phosphoimager.

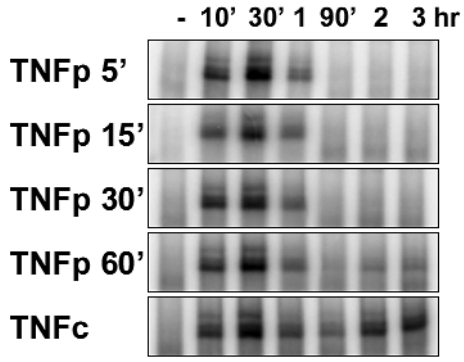

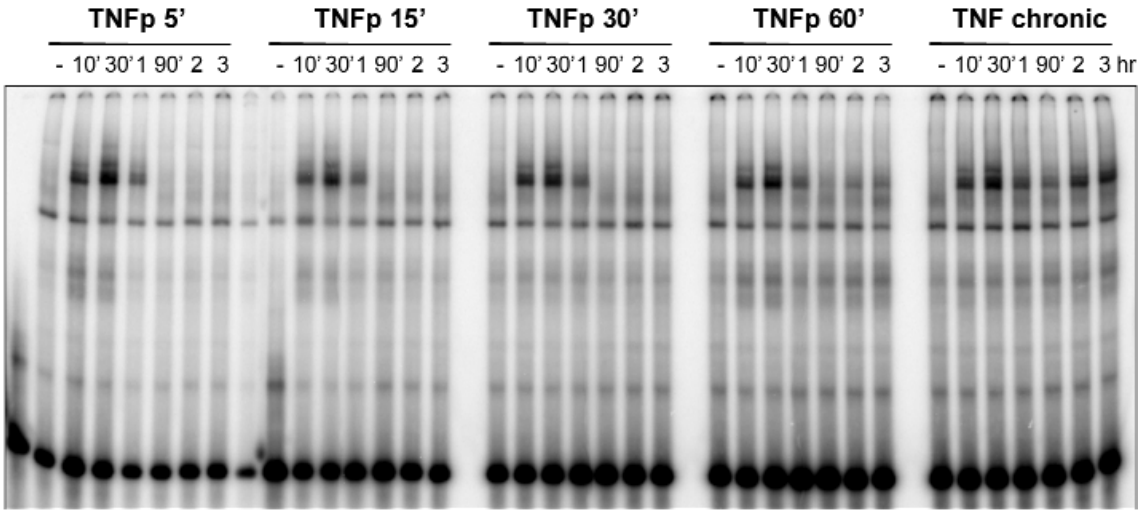

The IκB-NF-κB Signaling Module: Temporal Control and Selective Gene Activation

Alexander Hoffmann, Andre Levchenko, Martin L. Scott and David Baltimore

Science **298** (5596), 1241-1245.
DOI: 10.1126/science.1071914